Naufer et al., https://doi.org/10.1083/jcb.201702179

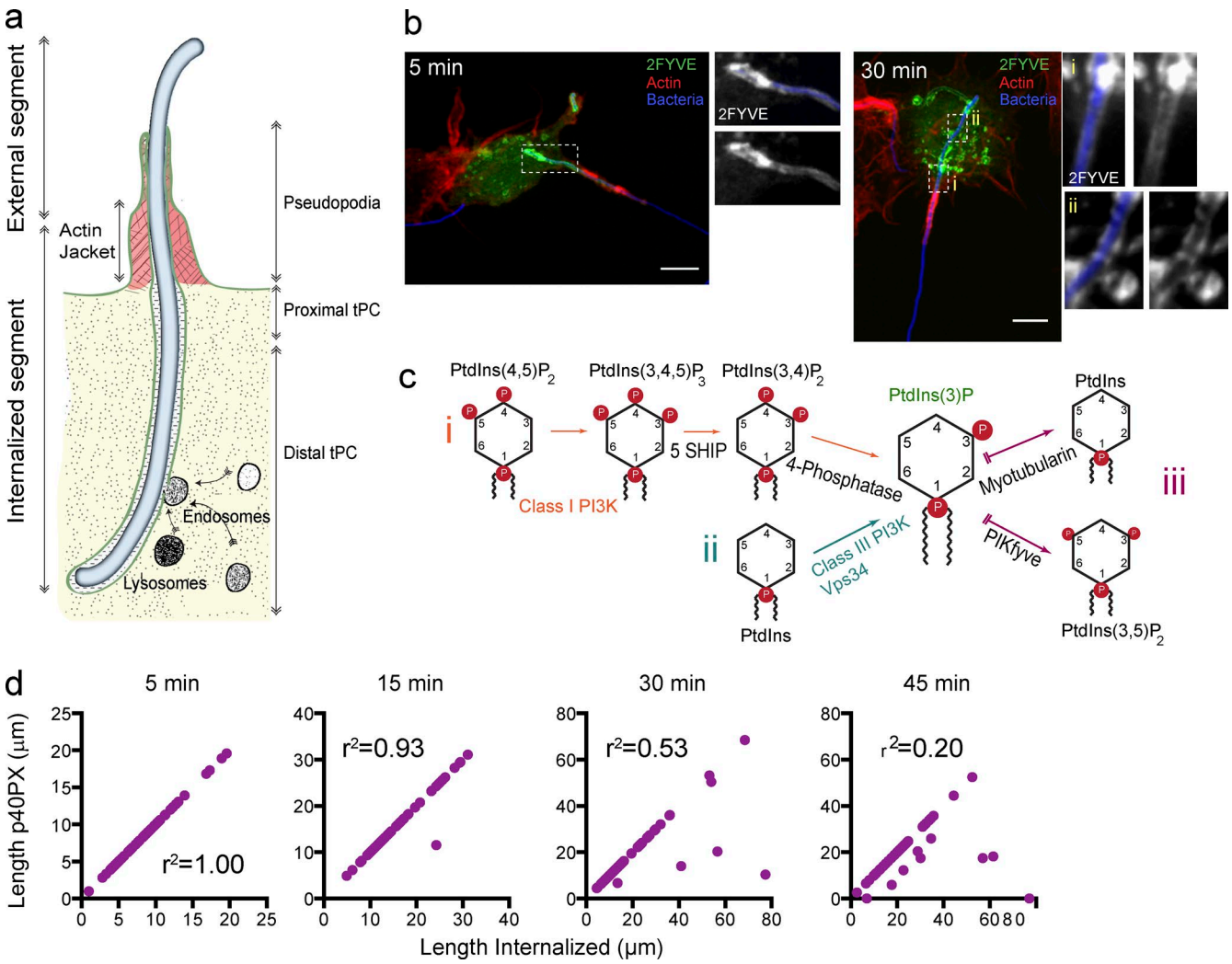

Figure S1. **PtdIns(3)P probes distribution in tPC.** (a) Schematic of the tPC formed during the uptake of filamentous bacteria based on Prashar et al. (2013). As macrophages ingest a filament, the cell extends pseudopodia, which, propelled by actin polymerization, advance along the target to form a phagocytic cup. Tracking within the growing pseudopodia, actin fibers form a dense jacket around the bacteria, forming a barrier that restricts permeability to large molecules (>10 kD) within the lumen of the phagocytic cup. The tPC is formed by infolding of the plasma membrane below the actin jacket (proximal tPC region), and it subsequently elongates to accommodate the length of the incoming filamentous target (distal tPCs region). (b) Longer tPCs tend to be partially decorated with PtdIns(3)P probes. 2FYVE-GFP recruitment to the base of tPCs. Actin jackets, denoted by F-actin accumulation (red), delineate the upper border of the phagocytic cup. Insets: magnified single plane from framed regions in the main panels. Bars, 5 µm. (c) Schematic of possible pathways for PtdIns(3)P production at tPCs. (i) PtdIns(3)P production may be mediated by class I PtdInsP 3-kinases in concert with PtdInsP 5- and PtdInsP 4-phosphatases. (ii) PtdIns(3)P may be produced by class III PtdIns 3-kinase from PtdInsPs. (iii) PtdIns(3)P turnover by myotubularins and PIKfyve. (d) RAW macrophages expressing p40PX-GFP were challenged with filamentous bacteria and fixed after 5, 15, 30, and 45 min of phagocytosis. The length of filamentous bacteria positive for p40PX-GFP was plotted against the bacterial length internalized at each time point. The corresponding correlation coefficient (r^2) was then calculated.

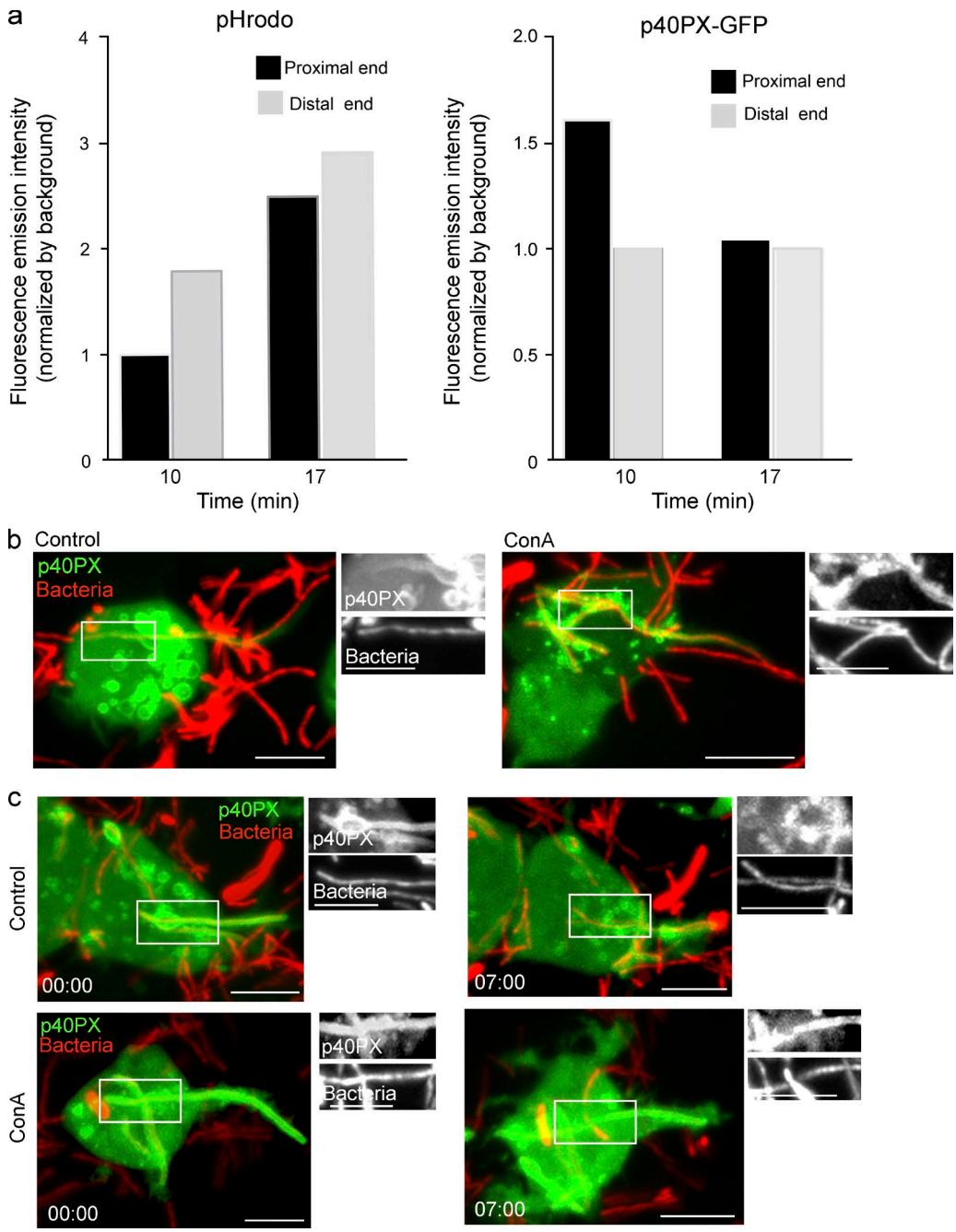

Figure S2. **Luminal acidification controls PtdIns(3)P distribution in the tPC.** (a) Loss of PtdIns(3)P is correlated with the acidification of tPCs. p40PX-GFP and pHrodo fluorescence emission were measured in selected frames from Video 2 (related to Fig. 5). pHrodo (left) and p40PX-GFP (right) fluorescence emissions recorded at the distal and proximal ends of the bacteria partially internalized in the tPC (10 min) or fully internalized in the newly formed phagosome (17 min). The data shown are mean intensities measured along 10 µm segments, in the distal and proximal ends, normalized by background fluorescence. (b and c) ConA treatment causes PtdIns(3)P retention in tPCs. RAW macrophages expressing p40PX-GFP (green) were left untreated or exposed to 1 µM ConA before being challenged with filamentous bacteria (red). (b) Elongated tPCs remained labeled with p40PX-GFP in ConA-treated cells, whereas distal tPCs were divested of the probe in control cells. (c) In control cells, p40PX-GFP was recruited to tPCs and dissociated upon enclosure of the bacteria into a phagosome (marked at 7 min). In ConA-treated macrophages, phagosomes remained labeled with p40PX-GFP (marked at 7 min). Bars, 5 µm.

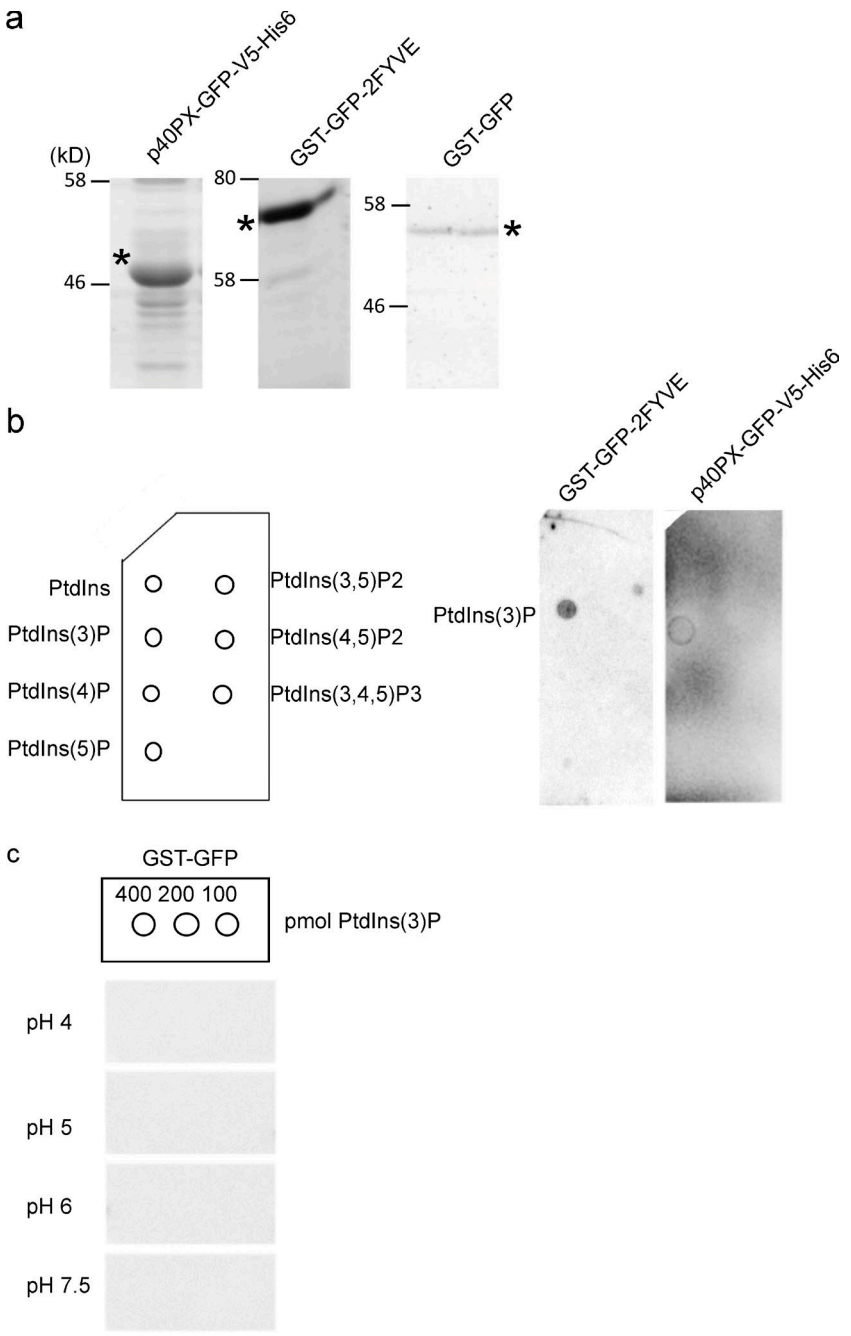

Figure S3. **Recombinant GST-GFP-2FYVE and PX-GFP-V5-His6 bind specifically to PtdIns(3)P.** (a) Recombinant GST-GFP-2FYVE, PX-GFP-V5-His6 and GST-GFP fusion proteins. Purification was done as described in the Materials and methods section. An aliquot from the final step of purification was analyzed by SDS-PAGE gel and proteins visualized with 2,2,2-trichloroethanol. Recombinant proteins are highlighted with an asterisk: GST-GFP-2FYVE (Molecular mass of 71 kD); PX-GFP-V5-His6 (47 kD); GST-GFP (53 kD). (b) The indicated phosphoinositides (200 pmol) were spotted on nitrocellulose membranes, and protein lipid overlays were performed using 0.5 µg/ml GST-GFP-2FYVE or PX-GFP-V5-His6 recombinant protein preparations. (c) Protein lipid overlay using 5 µg/ml GST-GFP control protein was performed at the indicated range of pH. In all blots, proteins bound to lipids were detected using anti-GFP antibody as indicated in the Materials and methods section.

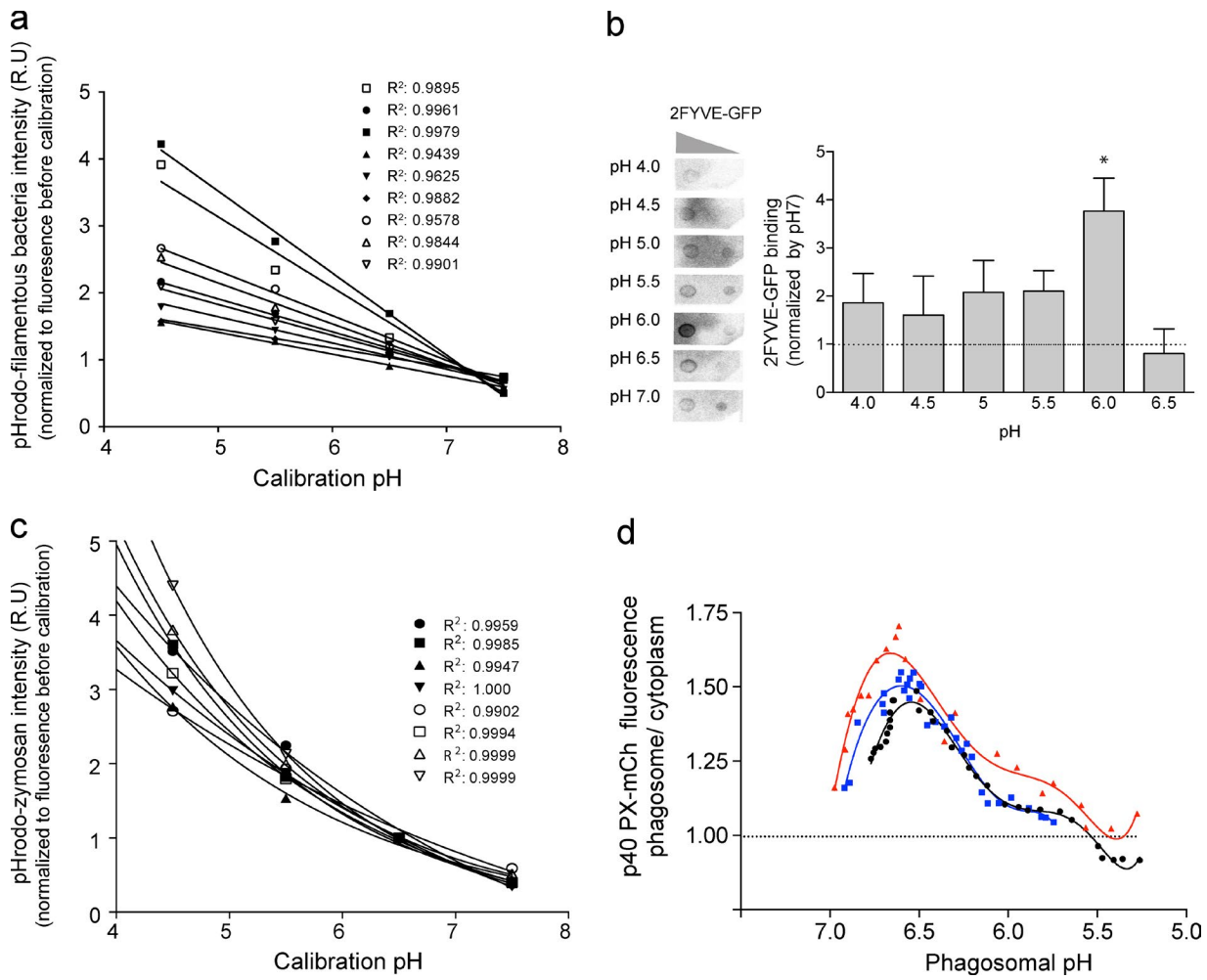

Figure S4. **Phagosomal pH calibrations and PtdIns(3)P probes response to pH.** (a) Representative pH calibration curves for 8 independent *Legionella*-containing phagosomes. pH calibrations were performed as described in the Materials and methods section. The corresponding fluorescence emission for phRodo-conjugated filamentous bacteria at each pH was normalized to the initial phagosomes fluorescence intensity (each value was corrected by background subtraction). The normalized values were plotted against their corresponding pH value, represented as relative units (R.U) and fit to a linear function. The corresponding R^2 values were determined. (b, left) Protein-lipid overlay (PLO) using recombinant GST-GFP-2FYVE and membranes containing 400 and 200 pmols of PtdIns(3)P. Representative experiment of three independent experiments performed with different preparations of recombinant protein. (Right) Densitometry of spots from each PLO expressed relative to that observed at pH 7 from three independent experiments. Results expressed as mean ± SEM (*, $P < 0.1$). (c) Representative pH calibration curves for 8 independent zymosan-containing phagosomes. pH calibrations were performed as described in panel a. For zymosan-containing phagosome pH calibrations, each curve was fit to a one-phase exponential decay function, and the corresponding R^2 values were determined. The function was used to determine the pH of the phagosome for that series. (d) Relationship between phagosomal pH and p40PX-mCh in zymosan-containing phagosomes. Data represent three independent phagosomes followed over 30–40-s intervals for 15 min.

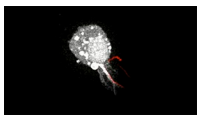

Video 1. **PtdIns(3)P dynamics in tPCs.** Phagocytosis of filamentous bacterial (red) by a RAW macrophage expressing 2FYVE-GFP (white). Target attachment to macrophages was synchronized (see Materials and methods), and cells were then moved to a microscope stage acclimatized for standard tissue culture conditions. Cells undergoing phagocytosis were identified and the selected frames were acquired every 20 s. Live cell imaging was obtained by simultaneous acquisition of both fluorescence channels in a spinning disk confocal microscope. The still frames in Fig. 4 a are related to Video 1.

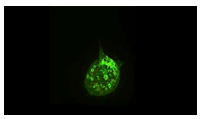

Video 2. **tPC acidification is correlated with the loss of PtdIns(3)P.** Macrophage cell expressing p40PX-GFP (green) undergoing phagocytosis of a pHrodo-conjugated filamentous bacteria. pHRodo fluorescence (red) is initially low throughout the tPC but increases in the distal end of the tPCs as it acidifies, while remaining low in the proximal tPC. As the tPC becomes a phagosome, pHrodo fluorescence becomes intense throughout. Frames from Video 2 were extracted to produce the micrographs from Fig. 5 (top row) and Fig. S2 a.

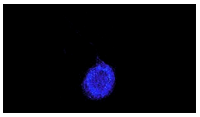

Video 3. **pHrodo signal transformed into a pseudo-color scale.** pHrodo signal transformed into a pseudo-color scale to help visualize changes in pHrodo fluorescence. Low pHrodo fluorescence emission, blue in rainbow palette, indicates a neutral pH, whereas high fluorescence emission is shown as red and indicates acidification. Live cell images were obtained by simultaneous acquisition of both green and red channels, using a spinning disk confocal microscope. Image frames were acquired every 25 s.

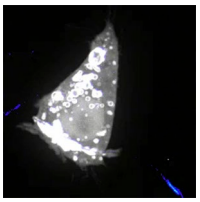

Video 4. **Exposure to acidic media induces the loss of PtdIns(3)P in tPCs.** RAW cells expressing p40PX-GFP (white) were presented with pHrodo bacteria (rainbow) at a neutral pH. Attachment was synchronized and cells were then moved to a prewarmed microscope stage (37°C). At 15 min after the onset of phagocytosis (T0), the external media was acidified to pH 4.5 and images were acquired by time-lapse confocal microscopy for every 30 s. Low pHRodo fluorescence emission, corresponding to neutral pH, is depicted as blue in the rainbow palette. High pHRodo fluorescence emission is shown in red and indicates acidic conditions. Frames from Video 4 were extracted to produce the micrographs from Fig. 6.

Reference

Prashar, A., S. Bhatia, D. Gigliozzi, T. Martin, C. Duncan, C. Guyard, and M.R. Terebiznik. 2013. Filamentous morphology of bacteria delays the timing of phagosome morphogenesis in macrophages. *J. Cell Biol.* 203:1081–1097. https://doi.org/10.1083/jcb.201304095